Molecular Neurobiology (2019) 56:2855–2869
https://doi.org/10.1007/s12035-018-1253-z

Alternative Splicing of the Delta-Opioid Receptor Gene Suggests Existence of New Functional Isoforms

Marjo Piltonen[1,2] · Marc Parisien[1,2] · Stéphanie Grégoire[1,2] · Anne-Julie Chabot-Doré[1,2] · Seyed Mehdi Jafarnejad[3] · Pierre Bérubé[4] · Haig Djambazian[4,5] · Rob Sladek[4,4] · Geneviève Geneau[5] · Patrick Willett[5] · Laura S. Stone[1,2,6,7] · Svetlana A. Shabalina[8] · Luda Diatchenko[1,2,6,7]

Received: 25 April 2018 / Accepted: 17 July 2018 / Published online: 31 July 2018

Abstract

The delta-opioid receptor (DOPr) participates in mediating the effects of opioid analgesics. However, no selective agonists have entered clinical care despite potential to ameliorate many neurological and psychiatric disorders. In an effort to address the drug development challenges, the functional contribution of receptor isoforms created by alternative splicing of the three-exonic coding gene, *OPRD1*, has been overlooked. We report that the gene is transcriptionally more diverse than previously demonstrated, producing novel protein isoforms in humans and mice. We provide support for the functional relevance of splice variants through context-dependent expression profiling (tissues, disease model) and conservation of the transcriptional landscape in closely related vertebrates. The conserved alternative transcriptional events have two distinct patterns. First, cassette exon inclusions between exons 1 and 2 interrupt the reading frame, producing truncated receptor fragments comprising only the first transmembrane (TM) domain, despite the lack of exact exon orthologues between distant species. Second, a novel promoter and transcriptional start site upstream of exon 2 produces a transcript of an N-terminally truncated 6TM isoform. However, a fundamental difference in the exonic landscaping as well as translation and translation products poses limits for modelling the human DOPr receptor system in mice.

Keywords Delta-opioid receptor · OPRD1 · Alternative splicing · Truncated receptor · GPCR

Introduction

The delta-opioid receptor (DOPr) is one of the four members of the opioid receptor (OR) family. DOPr is endogenously targeted by enkephalins which are opioid peptides. Currently, no clinically relevant selective drugs target it despite recognized potential for chronic pain, migraine, depression, anxiety, substance abuse, and some neurodegenerative conditions [1–3]. This creates an opportunity for drug discovery and development as delta-opioid drugs generally have a more favorable adverse effect profile (reduced potential for abuse, tolerance, respiratory depression, and constipation)

Electronic supplementary material The online version of this article (https://doi.org/10.1007/s12035-018-1253-z) contains supplementary material, which is available to authorized users.

✉ Luda Diatchenko
luda.diatchenko@mcgill.ca

[1] Faculty of Dentistry, Montreal, Quebec H3A 0G1, Canada

[2] Alan Edwards Centre for Research on Pain, McGill University, Montreal, Quebec H3A 0G1, Canada

[3] Goodman Cancer Research Centre and Department of Biochemistry, Faculty of Medicine, McGill University, Montreal, Quebec H3A 1A3, Canada

[4] Departments of Human Genetics and Medicine, Faculty of Medicine, McGill University, Montreal, Quebec H3A 0G1, Canada

[5] McGill University and Génome Québec Innovation Centre, Montreal, Quebec H3A 0G1, Canada

[6] Department of Anaesthesia, McGill University, Montreal, Quebec H4A 3J1, Canada

[7] Department of Pharmacology and Therapeutics, Faculty of Medicine, McGill University, Montreal, Quebec H3G 1Y6, Canada

[8] National Center for Biotechnology Information, National Library of Medicine, National Institutes of Health, Bethesda, MD, USA

compared to classic opioids like morphine that primarily act through the mu-opioid receptor (MOPr) [4, 5].

The canonical DOPr is a 7-transmembrane (7TM) spanning G-protein coupled receptor (GPCR) coded by three exons of the *OPRD1* gene. When activated, DOPr triggers several intracellular signaling pathways (reviewed in [6]), such as the classic $G_{\alpha i/o}$-protein complex-associated pathway and interactions with beta-arrestins 1 and 2. The expression of newly synthesized DOPrs on the plasma membrane depends heavily on N-glycosylation as well as palmitoylation [7, 8]. While two distinct DOPr pharmacological profiles have been described [9] and subsequently confirmed in multiple experiments, their molecular origins have remained unsolved [6]. Post-translational modifications, heteromerization, biased signaling, and alternative splicing have been proposed to explain their existence [10].

Alternative splicing presents an intriguing determinant in receptor diversity because it can lead to profound structural alterations of the receptor, affecting ligand selectivity, signaling, and trafficking. For example, the closest family member, mu-opioid receptor (MOPr) gene *OPRM1*, has at least 19 exons (some with multiple splicing sites) shuffled into over 30 transcripts in humans, and in mice, at least 18 exons are combined into over 50 transcripts (NCBI-RefSeq, Ensembl, UCSC Genome Browser). These transcripts code for three types of receptor isoforms: full-length 7TM receptors with varying C-termini, N-terminally truncated 6TM receptors, and highly truncated N-terminal 1TM fragments, which all have distinct characteristics and functions [11, 12]. The transcriptional landscape of *OPRD1* differs strikingly from *OPRM1*: so far, only one alternative transcript has been reported in mice and humans. The mouse variant codes for a putative 1TM fragment with no known function [13] while in the human variant, the third intracellular loop is abolished due to a 144-nucleotide cleavage through an unconventional mRNA processing mechanism that creates a receptor to inhibit the wild-type DOPr signaling [14, 15].

We hypothesized that the transcriptional variation of human *OPRD1* and mouse *Oprd1* is more diverse than currently known and is a source for multiple receptor isoforms. We describe novel functional alternatively spliced *OPRD1*/*Oprd1* variants coding for truncated receptor isoforms and present support for their functional significance by evolutionary conservation analysis and studies on context-dependent expression in selected tissues and mouse models. Ribosomal footprints on *OPRD1*/*Oprd1* provided us with evidence for translation of the new receptor isoforms. Our study also highlights a fundamental difference in the translation of certain receptor isoforms between mice and humans.

Methods

Cell Culture and Drug Treatments The BE(2)-C human neuroblastoma cell line (ATCC no. CRL-2268) was maintained in DMEM/F12 supplemented with 10% fetal bovine serum and penicillin–streptomycin (100 U/100 μg per ml). For the drug treatments, cells were seeded on a six-well plate at a density of 250,000 cells per well and left to attach overnight. The following day, growth medium was replaced with 100 nM [D-Ala2]-Deltorphin II (Tocris Bioscience, UK) in fresh medium, and the cells were incubated with the drug for 1 h to acutely upregulate DOPr-1 expression (based on a pilot project, data not shown). After incubation, the cells were collected in 1 ml of Qiazol lysis reagent (Qiagen Sciences, Germantown, MD, USA), pipetted back and forth to shear the cells, and stored at − 80 °C until RNA extraction.

Animals Male C57BL/6 and CD-1 mice (Charles River Laboratories, St-Constant, QC, Canada) were housed with a 12-h light/dark cycle in a temperature-controlled room in groups of two to five in individually ventilated polycarbonate cages, where they had free access to standard laboratory chow (2092X Global Soy Protein-Free Extruded Rodent Diet, Irradiated), corncob bedding (7097, Teklad Corncob Bedding, Envigo, UK), cotton nesting squares for enrichment, and water ad libitum. The mice were habituated to the housing conditions for at least 1 week before experiments. Experimental procedures were approved by the Animal Care Committee at McGill University and conformed to the ethical guidelines of the Canadian Council of Animal Care and the guidelines of the Committee for Research and Ethical Issues of the International Association for the Study of Pain. For naïve mouse tissues, three male C57BL/6 mice were sacrificed and decapitated under isoflurane anesthesia. Spinal cord, dorsal root ganglia (DRG), and various regions of the brain were dissected. All tissue samples were flash frozen on dry ice and stored at − 80 °C until RNA extraction.

RNA Extraction RNA from BE(2)C cells was extracted using a standard guanidinium thiocyanate-phenol-chloroform procedure. Sample tubes containing 1 ml of lysed cells in Qiazol were thawed, and 200 μl of chloroform was added to each tube and vortexed well. Phase separation was done by centrifuging the samples at 4 °C, 12,000×*g* for 15 min. The aqueous phase was carefully transferred to a clean microcentrifuge tube and mixed with 500 μl of isopropanol, incubated for 10 min at room temperature, and centrifuged again to pellet the RNA. The pellet was washed with 1 ml of 75% EtOH and re-precipitated by centrifuging at 4 °C, 7500×*g* for 5 min. The air-dried pellet was dissolved in 30 μl of RNAse-free, DEPC-treated water and heated for 10 min at 60 °C to fully dissolve and denature the RNA.

Frozen mouse tissues were immersed in 1 ml of Qiazol lysis reagent (Qiagen Sciences, USA) and homogenized using the Precellys 24-bead beater at 2 × 20 s at 5000 rpm (Bertin Technologies, France) or a rotating pestle. RNA was extracted using column purification kits (AllPrep DNA/RNA Mini Kit [spared nerve injury (SNI) mouse samples] or Qiagen RNeasy Lipid Tissue Mini Kit [all other mouse tissues], Germany) according to manufacturer's instructions included in the kit. Quality of RNA was examined with an Agilent Bioanalyzer or Nanodrop 2000 (Thermo Fisher Scientific) spectrophotometer, and any samples with values lower than RIN 8.4 or 260/280 1.8 were discarded.

5′RACE and Sequencing of the Products Rapid amplification of cDNA ends (RACE) was employed to discover previously unknown exons upstream of exon 2 in BE-(2)C cells, human brain, and mouse spinal cord. RACE-ready cDNA was created with the SMARTer RACE kit (Clontech, USA), and PCR was performed as instructed in the kit. Nested PCR was performed to increase specificity and to ligate adaptor sequences for further barcoding of the samples. For primers used in 5′RACE, please refer to the supplementary materials (Tables S1–S2). An aliquot of each nested reaction was run on a 1.2% agarose gel to verify the existence of amplified products, and the rest of the reaction was sequenced with PacBio RSII (in collaboration with Genome Quebec, Montréal, Canada).

PacBio RS II Sequencing The DNA libraries were prepared following the Pacific Biosciences 2 kb Template Preparation and Sequencing protocol. Between 200 and 750 ng of DNA were used for the library construction. The DNA damage repair, end repair, and SMRTbell ligation steps were performed as described in the template preparation protocol with the SMRTbell Template Prep Kit 1.0 reagents (Pacific Biosciences, Menlo Park, CA, USA). Samples were pooled at 3 nM for sequencing. The sequencing primer was annealed at a final concentration of 2.60 and 0.8333 nM. The P6 polymerase was bound at 1.5 and 0.50 nM. A portion of the bound complex 1.5 nM was added to the MagBeads bound complex for sequencing. The pool library was sequenced on a PacBio RSII instrument at a loading concentration (on-plate) of 10 to 40 pM using the MagBead OneCellPerWell v1 collection protocol, DNA sequencing kit 4.0, SMRT cells v3, and 4 h movies. The PacBio technology was used for this project because it eliminates the need to reconstruct the transcripts from short reads as it makes use of the proprietary SMRT bell library construction from the whole transcripts. Therefore, the exon junctions are preserved and precisely mapped. Even though the 5′RACE greatly increases the proportion of the desired transcripts, it is also possible to see non-amplified transcripts in the sample. The whole-transcript sequences were aligned with human and mouse genomes (hg19 and mm10, respectively).

cDNA Synthesis cDNA was synthesized from BE(2)-C and mouse RNA samples, as well as a collection of human nervous system RNAs (see Table S3; Clontech/Takara Bio, USA). In-lab extracted RNA was first treated with the TURBO DNA-free kit (Ambion/Thermo Fisher Scientific, USA) following the manufacturer's protocol. cDNA was synthesized with High-Capacity cDNA Reverse Transcription kit using 2 μg of RNA per 20 μl reaction (Applied Biosystems/Thermo Fisher Scientific, USA), Maxima RT kit using 5 μg of RNA per 25 μl reaction (Thermo Fisher Scientific, USA), or SuperScript™ III Reverse Transcriptase (Thermo Fisher Scientific, USA) using 1 μg per 20 μl reaction according to the instructions provided with the kits. A mock control sample without reverse transcriptase was prepared for all reactions.

RT-PCR To verify the transcription of putative new exons, PCR reactions were designed to amplify products spanning from the novel sequence over at least one exon-exon junction upstream or downstream of the exon, as well as down to exon 3. Reactions were prepared as specified in supplementary Table S4, and primers for each reaction are found in Tables S1–S2. PCR products were separated on a 1.5–2% agarose gel, visualized with ethidium bromide, and the bands of interest were cut out with a scalpel, purified, and eluted with a gel extraction column (QiaQuick Gel purification kit, Qiagen, Germany) for Sanger sequencing.

qPCR Relative transcript expression levels were determined with qPCR based on SYBR Green technology, except for the human exon 2b-a junction, which was analyzed with the PrimeTime® qPCR probe-based assay (Integrated DNA Technologies). cDNA template was mixed with SYBR Select Master Mix or TaqMan® Universal Master Mix II (Applied Biosystems/Thermo Fisher Scientific, USA; in the spared nerve injury experiment, SsoAdvanced™ Universal SYBR® Green Supermix) and appropriate primers. qPCR was run for 40–50 cycles according to the manufacturer's standard protocols found in the master mix kits on QuantStudio 7 Flex qPCR instrument (Applied Biosystems/Thermo Fisher Scientific, USA) or Rotor-Gene Q (Qiagen). Relative expression levels (ΔΔCt method, using priming efficiency e in the fold-change calculations; $e^{-\Delta\Delta Ct}$) were calculated using GAPDH as the reference gene and normalized to a suitable calibrator sample. For primers used in qPCR experiments, please refer to Tables S1–S2.

Potential outlier values were determined as a Ct value larger or smaller than group average ± 2xSD, but no value in any of the individual experiments fulfilled this criteria. Student's unpaired t test on ΔΔCt values was used to compare the changes in expression levels of each transcript in the spared nerve injury experiment (injury vs. sham) and repeated morphine experiment (morphine vs. control).

Evolutionary Analysis and OPRD1 Gene Architecture Multiple and pairwise comparisons and evolutionary rate estimation were performed for different functional domains of the gene using OWEN and MUSCLE alignments [16, 17]. Comparative pairwise analysis of mouse *Oprd1* exons was done with rat orthologous sequences (mm10, rn5), and human *OPRD1* exons were compared with macaque orthologues (hg38, rheMac3). Evolutionary divergence was estimated by PAML [18] in pairwise alignments for each exon of the *Oprd1* and *OPRD1* genes (Kn and Ks for coding; Ku for non-coding regions) for mouse–rat and human–macaque pairs. For each exon, multiple alignments of 60 (mouse) or 100 (human) vertebrate species were retrieved, with a 100-nt extension on both sides from the UCSC Genome Browser (http://genome.ucsc.edu). The conservation score of each exon was derived by averaging PhastCons scores ("Conservation Track") which measures conservation only such that "runs" of conserved sites are considered through the use of the hidden Markov model.

Ribosomal Profiling The GWIPS-Viz database [19] was used to detect translational activity within the *OPRD1* and *Oprd1* genes. Data on ribosomal footprints were collected from tracks in GRCh38/hg38 and GRCm38/mm10.

Spared Nerve Injury–Neuropathic Pain Model Male CD-1 mice were randomly assigned to groups for either SNI or sham surgery under isoflurane anesthesia at 10 to 12 weeks of age. In the SNI surgery, the left tibial and the common peroneal branches of the sciatic nerve were tightly ligated with 4-0 silk (Ethicon) and sectioned distal to the ligation, while sparing the sural nerve. In the sham surgery, the nerve was exposed without damaging it. Two weeks ($n = 8$ in sham, 9 in SNI) or 6 months later ($n = 8$ in both sham and SNI), animals were sacrificed by decapitation under isoflurane anesthesia and the frontal cortex was extracted, frozen on dry ice, and stored at − 80 °C until qPCR experiment. The hemispheres were pooled.

Repeated Morphine Treatment Male C57BL/6 mice were randomly assigned to receive either morphine sulfate 10 mg/kg (corresponding to 7.5 mg/kg morphine base; $n = 6$) or saline ($n = 5$) injected i.p. twice daily for 4 days, and all mice were challenged with morphine sulfate 10 mg/kg i.p. on day 5. Development of tolerance was verified with the tail-flick test (data not shown). After the experiment, the mice were decapitated under isoflurane anesthesia and the frontal cortex (pooled hemispheres) and spinal cord were extracted, frozen on dry ice, and stored at − 80 °C until use.

Accession Numbers Novel transcripts have been deposited with the GenBank under the following accession numbers: MG986890 (human DOR-1B), MG986891 (human DOR-1C), MG986892 (human DOR-1D), MG986889 (human DOR-1E), and MG986893 (mouse DOR-1E).

Results

Patterns of Alternative Splicing of *OPRD1*/*Oprd1* Genes Identified by 5′RACE

Our approach to discover previously unknown exons or splicing sites using 5′RACE PCR revealed a number of novel alternative transcripts in human *OPRD1* (Fig. 1a) in addition to the main transcript (Fig. 1b; Table S5). The most abundant alternative transcript DOR-1E contained an extended 5′ region of exon 2 with apparent multiple transcription start sites, but without exon 1 upstream (Fig. 1b; Fig. S1). This absence of exon 1 and stepwise pattern of the 5′ end of the new exon 2b suggests that DOR-1E has a new independent promoter. Furthermore, we identified two potential translation initiation codons that were in frame with the canonical DOPR sequence: one located 17 nucleotides upstream of exon 2a (at the end of exon 2b) and one 10 nucleotides (nt) away from the exon 2a junction (Fig. 1b; Table S5; Fig. S6–S7). DOR-1E is therefore a putative source of a truncated 6TM receptor isoform and can contain five unique N-terminal amino acids (aa) if translation starts from exon 2b. However, the first putative start codon in exon 2b lacks a significant Kozak consensus sequence nearby (no matching nucleotides at bolded positions: (gcc)gcc**R**ccAUG**G**), whereas the putative start codon in exon 2a is located near an adequate Kozak site (adenosine (A) at position R).

In three other alternatively spliced forms, DOR-1B, DOR-1C, and DOR-1D, a cassette exon surrounded by a consensus splicing pattern (AG/GU) was inserted between exons 1 and 2 (Fig. 1b; Fig. S1). In DOR-1C and DOR-1D, the additional exons (numbered 4 and 5) insert a premature termination codon (PTC) in frame with exon 1 more than 50–55 nt away from the last exon junction (exons 2 and 3), which makes them candidates for nonsense-mediated decay (NMD) [20]. Importantly, as the transcripts would undergo a pioneer round of translation before NMD, they simultaneously hold the potential to be source truncated 1TM fragments as described for MOPr transcripts SV1 and SV2 [21]. Finally, the 63-bp cassette exon 6 in DOR-1B does not contain an in-frame PTC but instead inserts 21 aa in to the first intracellular loop between the first and the second transmembrane domains without interruption of the canonical reading frame.

In the mouse, 5′RACE detected the main *Oprd1* transcript and a previously reported transcript, X1 (Fig. 2b) [13]. Transcript X1, also likely subjected to NMD due to a premature stop codon, can code for a 1TM receptor fragment. In an earlier study, this transcript was transiently expressed in cells and deemed non-functional [13]. In addition to these

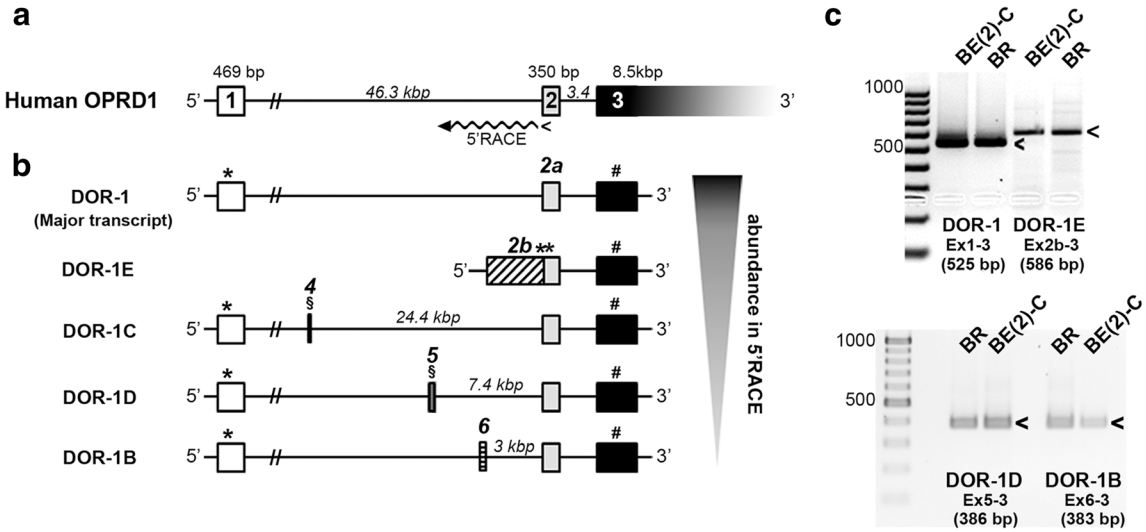

Fig. 1 Schematic representations of the human *OPRD1* gene and transcripts. **a** Current exonic structure of OPRD1, consisting of exons 1, 2, and 3. The 5′RACE PCR was primed from exon 2 (less than symbol, <), in the brain and BE(2)C cell line. **b** Five OPRD1 isoforms consistent with 5′RACE data. The canonical exon 2 in DOR-1 isoform is labelled 2a. New exons are labelled from left to right: exon 4 is in DOR-1C, exon 5 is in DOR-1D, exon 6 is in DOR-1B, and exon 2b is in DOR-1E. Isoforms are sorted by abundance, from most (DOR-1, major transcript) to least (DOR-1B). Canonical and putative in-frame translation start sites are marked with an asterisk (*), premature termination codons with a section mark (§), and canonical stop codons with a black number sign (#). **c** 3′ Extension of novel exons into constitutive exon 3. Extension was verified using PCR, in the brain (BR) and BE(2)-C cell line. Expected sizes in base pairs (bp) are shown for PCR products (less than symbol)

transcripts, we found a transcript with a 5′ extension of exon 2 resembling the human DOR-1E (Fig. 2b; Table S6). Interestingly, the first ATG in frame with the canonical DOR-1 sequence is in the middle of exon 2 and would be the initiation site of a very truncated receptor peptide. However, DOR-1E in mice could potentially be translated to a 6TM receptor by the use of a non-canonical start codon GUG at the end of exon 2b or even UUG in exon 2a located in the orthologous positions to human AUG codons (see comparative sequence analyses in Figs. S6 and S7).

The extension of the transcripts identified by 5′RACE to exon 3 was verified with RT-PCR. We successfully amplified all but one of the *OPRD1* transcripts (hDOR-1C), confirming that the exons 2–3 junction is found in all transcripts (Figs. 1c and 2c). Exon 4 of hDOR-1C, being derived from a repeat, was difficult to prime and led to contaminating PCR products. Since the complete sequence of mDOR-1E was already obtained by long-read sequencing, there was no need for further verification of exon junctions.

Evolutionary Conservation of *OPRD1*/*Oprd1* Alternative Splicing Events

To verify the newly identified human and mouse exons through evolutionary conservation, we delineated the exact boundaries and annotated them in different primates and

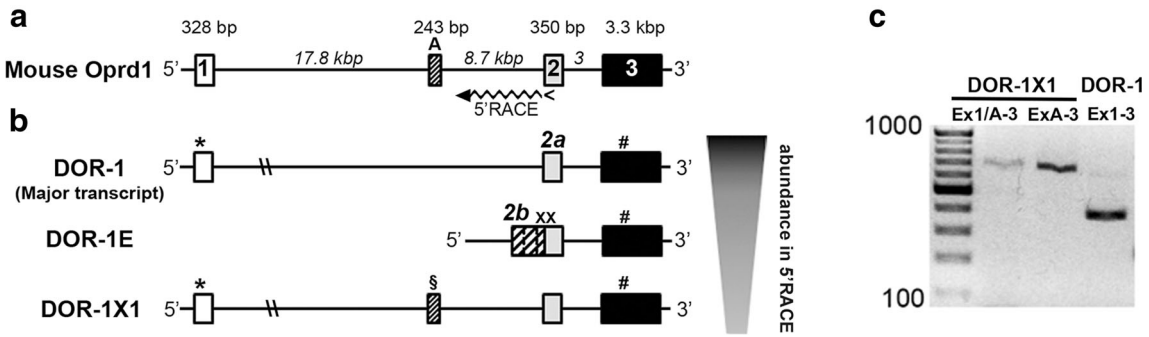

Fig. 2 Schematic representations of the mouse *Oprd1* gene and transcripts. **a** Current exonic structure of *Oprd1*, consisting of exons 1, 2, and 3. The 5′RACE PCR was primed from exon 2 (less than symbol, <) in the spinal cord. **b** -Three *Oprd1* isoforms consistent with 5′RACE data. The canonical exon 2 in DOR-1 isoform is labelled 2a. Alternative exons are labelled from left to right: exon A is in DOR-1X1, and exon 2b is in DOR-1E. Isoforms are sorted by abundance, from most (DOR-1, major transcript) to least (DOR-1X1). Canonical translation start sites are marked with a black asterisk (*), putative non-canonical start sites are marked with X, canonical termination codons are marked with a black number sign (#), and premature termination codons with a section mark (§). **c** 3′ Extension of novel exons into constitutive exon 3. Extension was verified with RT-PCR in spinal cord

rodent species using pairwise and multiple comparisons (Figs. S2–S5) and evolutionary rate estimation (Table 1a, b).

As expected, the level of similarity between constitutive exons 2–3 was significantly higher particularly in the coding region (phastCons 0.893–0.905 in humans and 0.889–0.917 in mice) compared to the newly identified alternative exons (phastCons 0.005–0.113 in humans, 0.023–0.172 in mice; see Table 1a, b). Interestingly, the intermediate level of conservation of exon 1 (phastCons 0.579 and 0.74 for coding sequence in humans and mice, respectively) suggested it is an alternative exon rather than a constitutive one. Nevertheless, this exon is ancient and belongs to the most common isoforms (in both humans and mice). The sequence similarity of exon 1 is significantly higher than of newly discovered alternative exons yet notably lower than in exons 2 and 3.

The pattern of similarity in human exon 2b is a mosaic of strength of conservation with significant similarity in the major parts of the exon between different mammals, especially primates. The 3′ end of exon 2b is highly conserved, and a very short open reading frame (ORF, 5 aa with conserved AUG at the beginning) continuing upstream of canonical exon 2 of the common *OPRD1* transcript was found in primates (see Figs. S6–S7). Comparative analysis of primates supports the possibility that the alternative transcript starting from exon 2b could be translated from the conserved AUG (17 nt from 3′ end of exon2b; see Figs. S6–S7) in the frame with the common *OPRD1* and code for the 6TM protein isoform. However, most of the exon 2b sequence comprises non-coding 5′ UTR, where the overall conservation is lower than in the 3′ end but some highly conserved elements such as AaCTgAAACT can be found, consistent with regulatory sites.

The newly discovered exon 2b in mice is not highly conserved with humans or other primates. However, the very short 3′ tail of these exons is conserved and overlaps with potential 6TM open reading frames in primates. Instead of AUG codons, GUG is found in the mouse and rat translation initiation position in exon 2b (see alignments in Figs. S6–S7). This position has a weak Kozak motif, as it is lacking the consensus nucleotides at the critical positions marked in bold: (gcc)gcc**R**ccAUG**G** (R can be A or G).

Finally, the multiple alignments around the exon 2a/b junctions (Fig. S7) reveal that nearly all vertebrates have a methionine codon either/both in exon 2a or 2b, establishing the theoretical possibility for a 6TM-DOPr translation from both sites. Mice do not have an in-frame methionine codon for 6TM DOPr in exon 2a or 2b but hypothetically may use non-canonical leucine (UUG) or valine (GUG) start codons [22, 23]. Unlike other vertebrates, the majority of rodents have

Table 1 Evolutionary comparison between (A) human–macaque and (B) mouse–rat OPRD1 exons. Acronyms are as follows: lenQ = length of sequence human (A) or mouse (B); lenS = length of sequence macaque (A) or rat (B); lenA = length of sequence considered for alignment; TT = number of transitions; TV = number of transversions; Ku = evolutionary rate at non-coding exons; Kn = evolutionary rate at nonsynonymous sites (CDS); Ks = evolutionary rate at synonymous sites (CDS)

A)	PhastCons score*	lenQ	lenS	lenA	TT	TV	Ku	Kn	Ks
Exon 1	0.308 ± 0.001	469	468	468	6	13	0.042	n/a	n/a
Exon 1/CDS	0.579 ± 0.003	227	227	227	3	5	0.036	0.0189	0.082
Exon 4	0.005 ± 0.001	118	85	85	8	16	0.370	n/a	n/a
Exon 5	0.113 ± 0.003	99	99	99	2	4	0.064	n/a	n/a
Exon 6/CDS	0.847 ± 0.009	63	63	63	0	3	0.050	0.0647	0
Exon 2b	0.087 ± 0.000	1656	911	911	20	48	0.079	n/a	n/a
Exon 2/CDS	0.905 ± 0.002	350	350	350	0	5	0.015	0.0089	0.010
Exon 3	0.136 ± 0.000	8526	7648	7599	114	332	0.062	n/a	n/a
Exon 3/CDS	0.893 ± 0.001	542	425	425	4	9	0.031	0	0.133
B)	PhastCons score#	lenQ	lenS	lenA	TT	TV	Ku	Kn	Ks
Exon 1	0.644 ± 0.002	328	328	328	7	17	0.078	n/a	n/a
Exon 1/CDS	0.740 ± 0.003	227	227	227	6	15	0.099	0.045	0.258
Exon A	0.023 ± 0.001	243	223	223	17	34	0.281	n/a	n/a
Exon 2b	0.172 ± 0.001	1760	1710	1627	70	146	0.148	n/a	n/a
Exon 2a	0.917 ± 0.001	350	350	350	5	14	0.057	0	0.27
Exon 3	0.393 ± 0.001	1267	1270	1250	39	99	0.121	n/a	n/a
Exon 3/CDS	0.889 ± 0.001	543	543	543	5	14	0.036	0.08	0.201

n/a not applicable

*PhastCons score is estimated based on multiple alignments of 100 species downloaded from UCSC browser

PhastCons score is estimated based on multiple alignments of 60 species downloaded from UCSC browser

a missense mutation of the first in-frame AUG in exon 2a to UUG or CUG and of the in-frame AUG at the end of exon 2b to GUG as is in mice (Fig. S7).

Among the novel cassette exons, the high level of similarity between human exon 4 and several closely related primates like the macaque (Figs. S2 and S3) is explained by the fact that this exon is an AluJb-like containing highly repeated sequence in the human genome. However, not all closely related primates and other vertebrates contain this sequence in orthologous positions. Thus, exon 4 may represent a mechanism of new exon origin from Alu repeats [24]. Conserved insertion of PTCs in frame with exon 1 by both exons 4 and 5 (Fig. S3) suggests that these newly discovered events might be involved in regulating gene expression levels through NMD. Exon 5 is highly similar to its orthologue in macaque (Figs. S2 and S3) but is not found in most known sequenced primate genomes. Thus, we can conclude that exon 5 is evolutionarily recent and does not contain a high protein coding potential.

An interesting exception among the new human cassette exons was the highly conserved alternative exon 6 (phastCons 0.847). Multiple alignments (Fig. S2) show this sequence is quite ancient, and the trace of similarity is seen in numerous vertebrates. Despite the high similarity of exon 6 in primates, the calculated protein level of selection was quite low (Kn > Ks; see Table 1a). This is an example of a new alternative coding exon originating from an ancient conserved non-coding sequence, not interrupting the ORF of the common *OPRD1* transcript, and inserting 21 aa into the first intracellular loop.

Comparative analysis of exon A in mouse *Oprd1* showed that it is highly conserved only between mice and rats (Figs. S4 and S5) especially at the 5′ end of the exons, presenting a similar related species-specific conservation as seen with alternative human exons only among primates. Exon A contains PTCs in DOR-1X1 transcripts in both mice and rats, although the positions of the PTCs are slightly different in the alignments (Fig. S4). Since the PTC is located 50–55 nt away from the last exon junction, the 1 × 1 transcripts may be subject to elimination by NMD [20], similar to human variants DOR-1C and DOR-1D.

Relative Expression Levels of *OPRD1*/*Oprd1* Transcripts in CNS and Fetal Tissue

We next estimated the expression levels of the major and alternative transcripts in both human (Fig. 3) and mouse (Fig. 4) nervous system tissues. All transcripts were detected in the same tissues to varying degrees. In humans (Fig. 3a), the abundance of the alternative transcripts varied from the extremely low expression of DOR-1D (1/1000–1/10000-fold) to the relatively high levels of DOR-1E (up to 1/5) in comparison to the expression of the major transcript. The expression of alternative transcripts in different tissues generally paralleled that of the major transcript except for DOR-1D (Fig. 3b–f). We also studied the expression of DOR-1E (putative 6TM receptor) in multiple peripheral tissues with RT-PCR (Fig. S8) and observed it again mostly paralleled the expression of DOR-1. The most striking difference was seen in placenta, where DOR-1E was abundantly expressed, but no DOR-1 was detected. Leukocytes and spleen seem to express low levels of DOR-1E only, whereas skeletal muscle seems completely devoid of any DOPR expression.

In mice, the expression levels of DOR-1X1 were 3–23% of those of the main transcript, whereas DOR-1E was expressed a maximum of 10% of the main transcript levels in the nervous system (Fig. 4a). Again, the expression patterns of the alternative transcripts parallel the major isoform, except that DRG seem to display a much lower level of alternative splicing than the other nervous system tissues (Fig. 4b–d). We also examined the expression levels in the heart as DOPr has been implicated in cardio-protection, and we observed unusually high levels of alternative transcripts there compared to the nervous system tissues. However, the overall expression of DOPr in the heart is extremely low.

Interestingly, in both species, the frontal brain, striatum/caudate nucleus, and nucleus accumbens showed a relatively high expression of the alternative transcripts. One of the main species differences in the expression pattern was seen in the spinal cord: in mice, there is an abundance of DOPr transcripts, whereas in humans, the expression levels are very low.

Translation of DOR Isoforms from Human and Mouse Alternative Transcripts

To obtain evidence for the translation of alternatively spliced isoforms, we explored ribosomal footprints tracked in the GWIPS-Viz browser. In general, either the expression of human *OPRD1* is lower in the datasets included in the browser (GWIPS-Viz does not contain many libraries of human nervous system origin) or the sequencing depth is lower in comparison to data on mice. Nevertheless, in addition to the obvious ribosomal activity in exons 1, 2, and 3 (Fig. 5a), we observed ribosomal footprints at the junction of exons 2a and 2b indicative of ribosomal activity in DOR-1E (Fig. 5b). These data are mostly supportive of translation starting from the beginning of exon 2a, as footprints extending to cover the putative AUG start codon in exon 2b are not present. The ribosomal footprint begins 14 nt before the AUG in exon 2a and extends to exon 2b, which is consistent with the typical 13–15 nt offset distance that depends on the footprint length [25]. The human ribosomal footprints were derived from a study by Werner and colleagues [26] that profiled human embryonic stem cells having undergone embryogenesis for 6 days.

In mice, we observed strong peaks arising from the three canonical exons as expected and lower but distinct peaks on

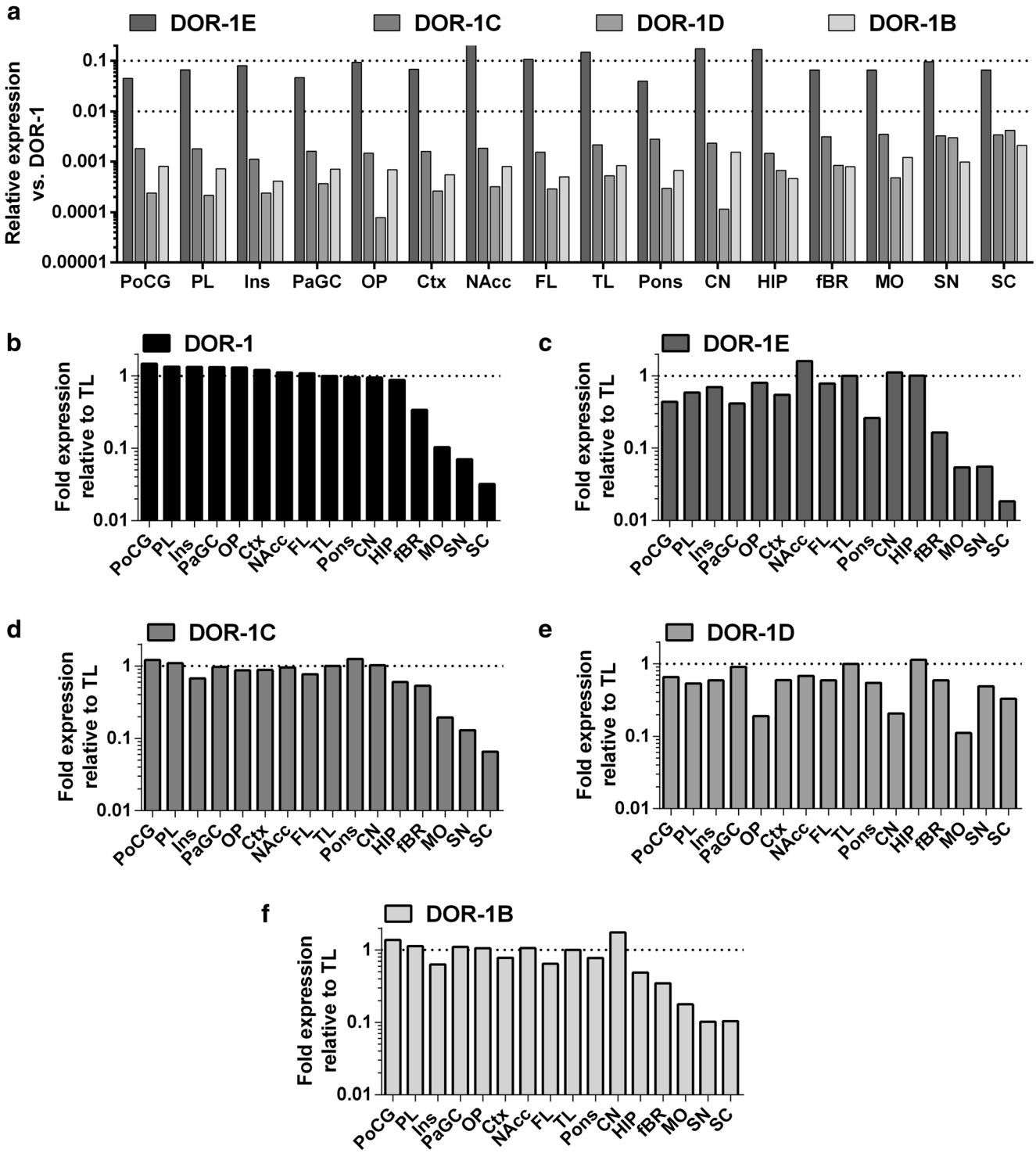

Fig. 3 Relative expression of DOR splice variants in the human nervous system tissues. The expression levels of DOR-1 and alternative transcripts were determined with qPCR. **a)** Expression levels of all human alternative transcripts, normalized against DOR-1 (fold expression = 1) in each individual tissue. **b–f** Relative expression levels of each transcript: **b** DOR-1, **c** DOR-1E, **d** DOR-1C, **e** DOR-1D, and **f** DOR-1B normalized to the transcript level in temporal lobe (TL, fold expression = 1). Note the logarithmic scale. Tissues are as follows: CN caudate nucleus, Ctx cerebral cortex, FL frontal lobe, HIP hippocampus, Ins insula, MO medulla oblongata, NAcc nucleus accumbens, OP occipital pole, PaCG para central gyrus, PL parietal lobe, PoCG post central gyrus, SN substantia nigra, TL temporal lobe, fBr fetal brain, SC spinal cord

exons A and 2b (Fig. 5c–e). Similar to human data, the junction of exons 2a and 2b, corresponding to DOR-1E, has low coverage (Fig. 5d). This supports our evidence from conservation analysis that mouse DOR-1E may be translated from an

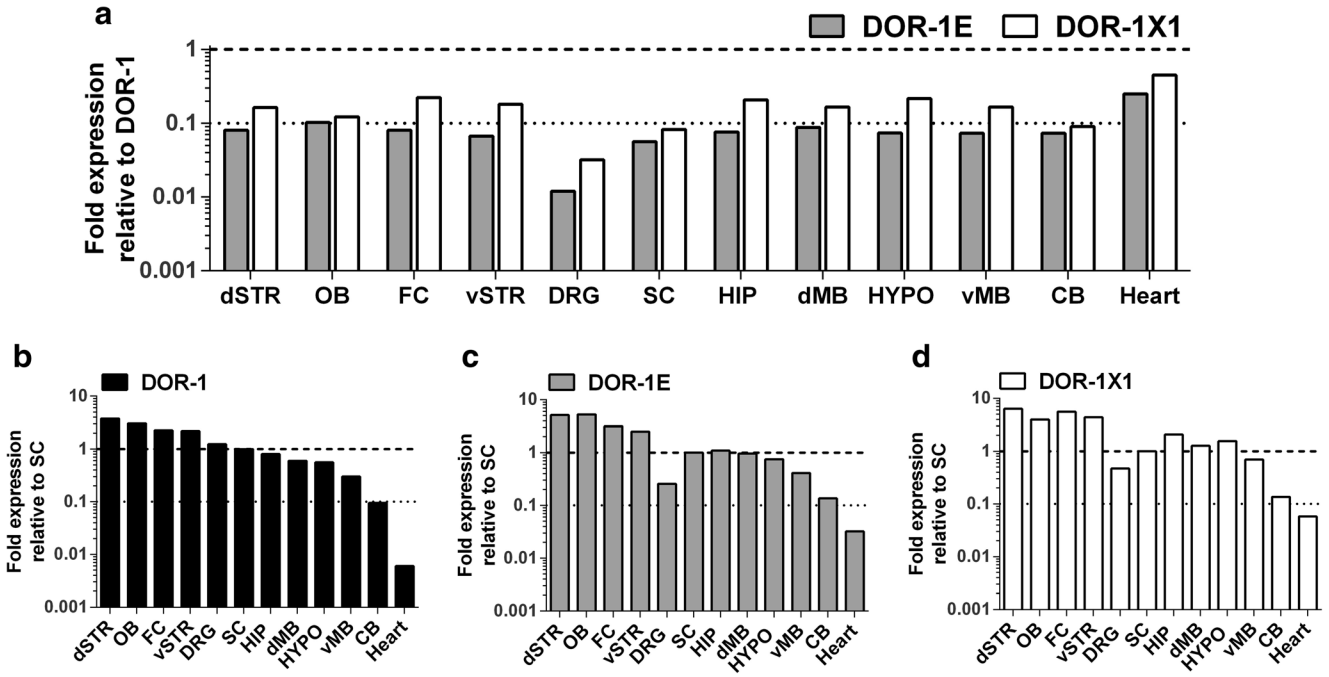

Fig. 4 Relative expression of DOR splice variants in the mouse nervous system and heart. The expression levels of DOR-1 and alternative transcripts were determined with qPCR. **a** Expression levels of the alternative transcripts, normalized against DOR-1 (fold expression = 1) in each individual tissue. **b–d** Relative expression levels of each transcript **b** DOR-1, **c** DOR-1E, and **d** DOR-1X1, normalized to the transcript level in spinal cord (SC, fold expression = 1). Note the logarithmic scale. Tissues are as follows: CB cerebellum, dMB dorsal midbrain, DRG dorsal root ganglia, dSTR dorsal striatum (incl. Caudate putamen), FC frontal cortex, HIP hippocampus, HYPO hypothalamus, OB olfactory bulb, SC spinal cord, vMB ventral midbrain (incl. ventral tegmental area, substantia nigra), vSTR ventral striatum (incl. nucleus accumbens)

alternative start codon, likely the UUG in exon 2a, because this footprinting begins 14 nt before the UUG codon. There is one read extending further into exon 2b as well, so we cannot exclude the possibility that the alternative initiation site in exon 2b can be used (Figs. S6–S7). Upon examination, the peak corresponding to exon A revealed that the ribosomal footprints were clustered towards the 5′ end and the middle of exon A and extended at maximum 36 nt past the in-frame stop codon. Only one read was seen located at the end of exon A. This provides evidence supporting the translation of 1TM-DOPr produced from the transcript DOR-1X1 in mice.

Expression of DOR-1X1 is Selectively Regulated in a Mouse Model of Chronic Pain

We next searched for a condition under which the levels of DOR-1E or DOR-1X1 would be regulated independently from the major transcript as further evidence for biological function of the alternatively spliced isoforms of DOPr. We studied the expression of DOPr isoforms in a chronic mouse pain model (SNI) and in mice treated with repeated morphine administration similar to paradigms producing tolerance, since DOPr is known to play a role in these conditions. There were no significant differences in the expression of DOR transcripts at 2 weeks post-SNI injury when compared to the sham-operated group (Fig. 6a). At 6 months post-injury, there was a selective 1.96-fold upregulation of DOR-1X1 but not DOR-1 or DOR-1E in the SNI group when compared to sham (Fig. 6b; $p < 0.05$, Student's unpaired t test on $\Delta\Delta$Ct values). In contrast, repeated morphine administration did not significantly change the expression of DOR transcripts either in the frontal cortex or the spinal cord (Fig. 6c, d). These results suggest that murine DOPr transcripts can be regulated independently of each other and suggest that they may have different functional properties.

Discussion

In this work, we showed that the transcription of human and mouse genes coding for DOPr is more complex than previously established. We observed the inclusion of cassette exons in both species in the major DOPr transcript, predicted to code for short 1TM peptides or to insert amino acids, and we observed a putative alternative transcription start site upstream of exon 2, potentially coding for the 6TM receptor isoform. This gene locus structure resembles that reported for *OPRM1* [11, 12]. Therefore, *OPRD1* transcripts, like *OPRM1*, hold a

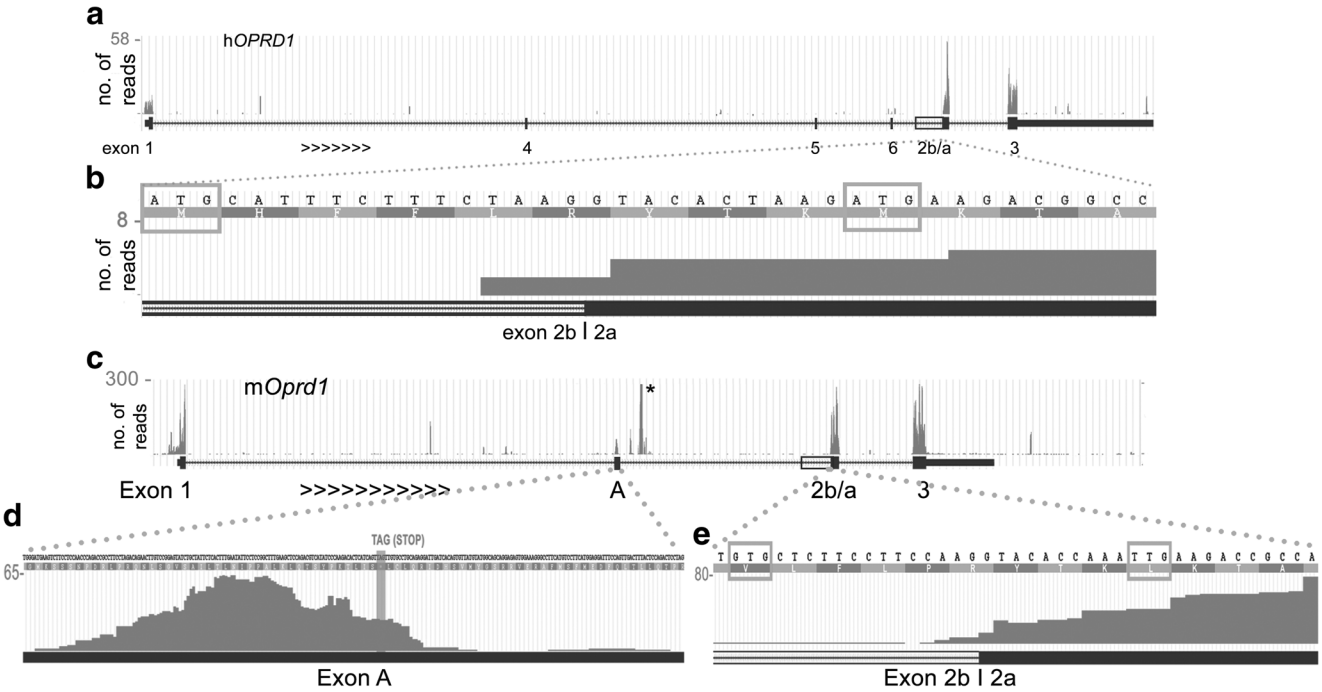

Fig. 5 Ribosomal footprints in human *OPRD1* and mouse *Oprd1*. Data from GWIPS-Viz browser, depicting sequencing read pileups of ribosomal footprints. **a** Ribosomal footprints on human *OPRD1* (hg38) show good coverage of exons 1, 2, and 3. **b** Ribosomal footprint extending to exon 2b of human *OPRD1*, indicating translation of DOR-1E from the methionine in exon 2a. Both putative start codons are highlighted with a box. **c** Ribosomal footprints on mouse *Oprd1* (mm10) show good coverage of exons 1, 2, 3, and exon A. Asterisk denotes a high peak aligning to tRNA alanine 5 (anticodon CGC) located on the positive strand, overlapping the *Oprd1* gene. **d** The ribosomal footprints in exon A generally do not cover the end of the exon but terminate at the vicinity of premature termination codon (marked with a vertical bar). **e** Ribosomal footprint extending to exon 2b of mouse *Oprd1*, indicating translation of DOR-1E, likely from exon 2a. Codons in boxes denote the non-canonical start codons orthologous to human ATG codons. Figures enlarged and annotated from screenshot from the GWIPS-Viz browser

similar potential to code for the truncated 1TM and 6TM receptor isoforms that contribute to a variety of cellular effects. In support of this, we have provided evidence both for translation of alternative DOPr isoforms and for selective regulation of the DOR-1X1 transcript in mice, highlighting its biological significance.

From a methodological aspect, 5′RACE was crucial for the transcript discovery due to their low abundance and challenging sequences. Consistent with this, we looked for alternative splice variants in numerous RNA-sequencing datasets covering human nervous system tissues but found only the major transcript while the mouse variants were inconsistently present in such data (results not shown). The same is true for the *OPRM1* gene: in spite of numerous evidence for multiple functional *OPRM1*, they are difficult to locate in the available RNA-sequencing datasets.

We next employed comparative genome analysis to obtain evidence for the evolutionary conservation of the new alternative exons. We observed conservation within closely related species with lower levels of similarity than constitutive exons. Not all of the analyzed human exons had corresponding orthologues within the mouse and rat *Oprd1*. This means the exons are subject to genetic variability that can modify receptor function and associated phenotypes in species specific manners [27, 28]. Low conservation of the cassette exons between species is in line with the work of Yan et al. whose systematic analysis of alternative splicing events in the mouse and human cortex concluded that the majority of low-abundance cassette exons in mice do not have an orthologue in humans [29]. This is also the case with alternative exons in *OPRM1* [11, 12, 30]. Evolutionarily, recent exons generally have low levels of expression, supported by our observations from RT-PCR and ribosome profiling experiments and in agreement with previous studies [31, 32].

It is also worth noting that two of the three human cassette exons and exon A in mice insert a PTC in the canonical reading frame starting from exon 1. The locations of the PTCs are such that the transcripts bearing these exons are strong candidates of NMD. Originally, NMD was considered a post-transcriptional surveillance mechanism to remove abnormal transcripts that could code for potentially deleterious proteins recognized by the cell as a major isoform [20], but a high proportion of NMD exons may directly control gene levels among other functions, especially in the brain [29, 33–35].

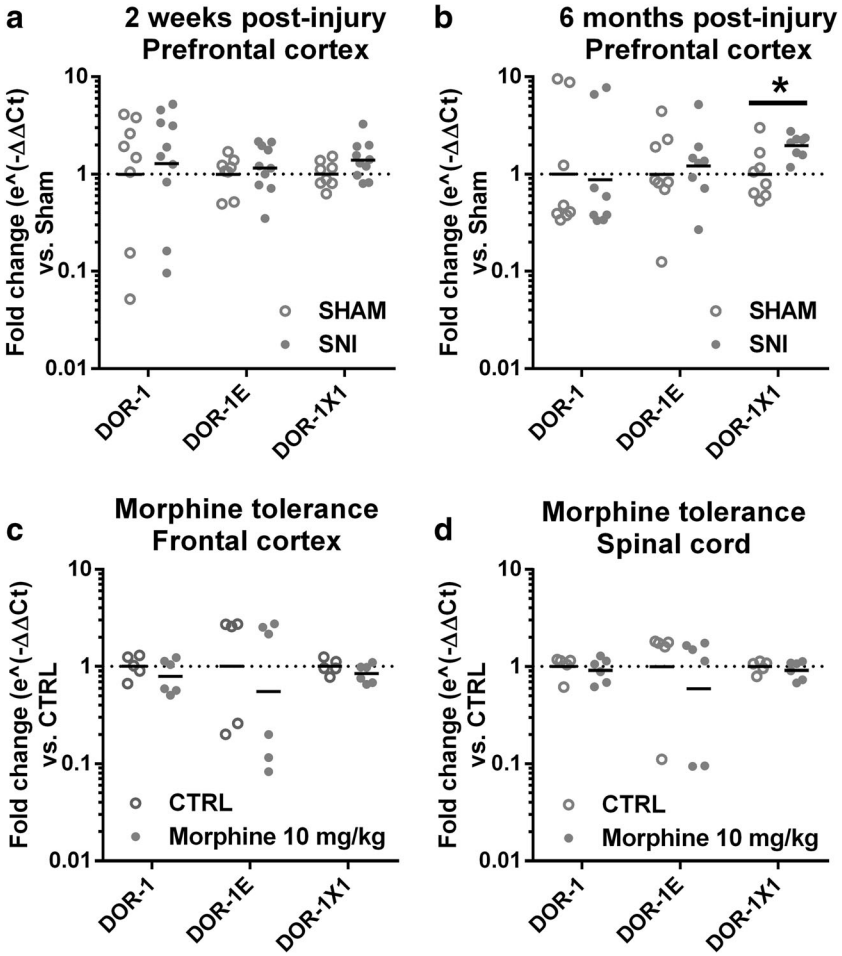

Fig. 6 Differential regulation of DOR transcripts in mice. DOR-1, DOR-1E, and DOR-1X1 transcript levels are contrasted between two conditions (open vs. filled grey circles) to highlight differential regulation. **a, b** Mice subjected to neuropathic pain model via spared nerve injury (SNI) compared with sham. There were no significant changes in the expression levels of DOR transcripts at 2 weeks post-SNI injury (**a**) when compared to the sham group. The expression of DOR-1X1 was significantly higher in the prefrontal cortex of the SNI group than sham-operated group (*$p < 0.05$) at 6 months after surgery (**b**), while levels of DOR-1 or DOR-1E were not affected. **c**, **d** Mice subjected to repeated administration of morphine compared to controls (CTRL). Morphine administration in mice did not significantly change the expression of DOR transcripts in the frontal cortex (**c**) or the spinal cord (**d**). Data were expressed as individual data points, and the geometric mean of each group is marked with a short solid black line

Because NMD requires a pioneer round of translation to recognize the in-frame PTC, the DOR isoforms with PTC-containing cassette exons can be translated into 1TM receptor fragments, as evidenced by ribosomal footprints. .

In terms of comparative genome analysis, DOR-1E is an especially interesting transcript as it lacks exon 1 and appears to have multiple transcriptional start sites located in exon 2b in humans and mice. This suggests that another promoter exists upstream of exon 2a, similar to *OPRM1* [30]. Although the DOR-1E transcripts in humans and mice are structurally similar, mice lack an AUG codon close to the 5′ end of exon 2a and upstream in exon 2b, unlike humans and majority of mammals. Because we found evidence of translational activity for this transcript in the mouse ribosomal footprints, an alternative initiation codon must be used in mice (in many other rodents as well), supported by expanding evidence of alternative initiation codons in both mice and humans. Mouse embryonic stem cells display a surprisingly frequent use of CUG, GUG, and UUG as initiating codons [22]. CUG is used to produce antigenic peptides for MHC I presentation in human cells [36, 37] and thioredoxin/glutathione reductase isoforms in mice [38]. GUG is an initiation codon for the human mitochondrial ATP6 gene [23], and ACG is used to translate the postsynaptic scaffold protein Shank1 in dendrites [39]. Further studies are required to elucidate the details of how the transcription and translation of DOR-1E is regulated.

In general, the *OPRD1* alternative isoforms were expressed with varying abundance alongside the major isoform in

nervous system tissues. Both DOR-1 and DOR-1E were expressed in numerous peripheral tissues in humans: there are tissues (placenta, leukocytes, spleen) with an abundance of DOR-1E while the canonical DOR-1 seems either absent or has very little expression. Alternative splicing is highly dependent on the context, such as tissue, developmental stage, cellular differentiation, or even external stimuli [40]. The brain has the highest proportion of alternatively spliced genes, followed closely by the testis and liver, whereas skeletal muscle and uterus show the lowest proportion of such genes [41].

Our results on ribosomal-protected mRNA fragments show that DOR-1X1, originally discovered by Gaveriaux-Ruff et al. [13], is a source of 1TM-DOPr in vivo. Although the previous study [13] demonstrated no DOPr ligand binding when DOR-1X1 cDNA was transfected into COS-cells, it may be worthwhile to re-evaluate its functionality. DOR-1X1 functionality may be revealed in co-expression studies with DOR-1 or other opioid receptors, as we know that a 1TM-MOPr functions as a chaperone in the endoplasmic reticulum to increase the expression of 7TM MOPr [42]. Furthermore, the ribosomal footprints show that DOR-1E is potentially a source of 6TM-DOPr in mice and humans. Unlike the 1TM DOPr variant, the 6TM potentially has a ligand-binding pocket but is likely to need a partner for trafficking similar to the 6TM-MOPr [43]. Since practically none of the canonical 7TM-MOPr ligands bind to 6TM-MOPr [44], we should expect similar ligand specificity for DOPr variants.

We showed that alternative splicing of *Oprd1* was selectively upregulated in the murine SNI pain model. Although the upregulation appears modest, it may be the result of a robust localized change in expression, as alternative splicing is known to be very tissue- and cell-type specific. The exact mechanism of how DOR-1X1 alone was upregulated in our SNI experiment remains to be addressed, though hypothetically may be attributed to epigenetic regulation as it is known to affect alternative splicing (reviewed by [45, 46]). In the well-characterized SNI model, two out of three branches of the sciatic nerve are ligated unilaterally and sectioned distal to the ligation, causing a rapid onset of mechanical allodynia reminiscent of neuropathic pain that persists for months without significant recovery [47]. The timeline of changes in expression in our experiment (6 months) parallels long-term rather than acute changes and is consistent with DNA methylation-dependent regulation of gene expression. This is also in agreement with experiments by Massart and co-workers demonstrating that SNI in rats for 9 months induces hypo-methylation of the *Oprd1* promoter and that more extensive hypo-methylation is associated with higher mechanical sensitivity [48]. A direct link of our finding to the Massart study cannot be made given that the latter screened the methylation status of the promoter, not the transcriptional changes. Nevertheless, functionally relevant changes in the methylation of the *Oprd1* promoter evolved during a comparable timeline to our experiment. It is also worth noting that the analgesic effectiveness of DOPr agonists in chronic inflammatory pain is attributed to increased trafficking of DOPr and enhanced functional coupling via multiple mechanisms [49]. Currently, we do not know how the expression of DOR-1X1 is affected by chronic inflammatory pain, or how neuropathic pain changes the trafficking of DOPr; the putative chaperone-like contribution of 1TM DOR-1X1 should be evaluated in both contexts.

Contrasting the SNI experiment, *Oprd1* transcript variant levels were not significantly changed in our paradigm for acute morphine tolerance, suggesting a context-dependent regulation of specific transcripts. In support, another study on repeated but short-lasting morphine administration (48 h) in rats also resulted in no changes in *Oprd1* gene expression [50]. However, studies on the effects of prolonged or chronic morphine administration on *Oprd1* expression are lacking.

Acknowledging the major challenges in making use of DOPrs as drug targets, it is essential to consider the contribution of these new receptor isoforms. According to our results, the genetic architectures of DOPr transcripts are similar to MOPr, including a 6TM transcript with an extended 5′ region of exon 2 with multiple transcription start sites. This suggests that like MOPr, DOPr has an alternative promoter in this region. Therefore, 6TM-MOPrs provide a relevant example of an alternative receptor isoform as a potential drug target [12, 43, 44]. Initially, because of low expression and a substantial truncation, their functionality was questioned [51]. In vitro studies indicated that 6TM-MOPrs are functional receptors and produce excitatory rather than inhibitory cellular effects in comparison to 7TM MOPrs [43, 52, 53]. 6TM-MOPr also needs to heterodimerize with other receptors such as beta2-adrenoceptor or NOP to be efficiently transported to the plasma membrane [43, 44]. Animal studies suggest that 6TM-MOPrs not only could be targets for analgesics but also contribute to opioid tolerance, dependence, and opioid-induced hyperalgesia, which are concerning issues in long-term opioid treatment [43, 54, 55]. Less is known about the 1TM-MOPr fragments, apart from their chaperone role, facilitating proper folding of 7TM MOPrs in the endoplasmic reticulum and thus increasing receptor stability [42]. Additionally, knocking down a specific 1TM-MOPr variant in mice reduced morphine analgesia by approximately 50% [42]. Since *OPRD1* appears to code for structurally similar receptor variants, their functional contribution should be carefully considered.

Finally, our study bears important implications concerning mice as experimental animals to model receptor systems. Indisputably, mice are essential for biomedical studies. However, we provide an example of a receptor gene that is structurally similar in mice and humans, but differs in sequence conservation at the level of alternative splicing, and importantly, differs in translational

mechanism. While the human 6TM-DOPr can be translated using a canonical start codon, in mice, the use of a non-canonical start is necessary. Therefore, it is likely that very specific and different external and intracellular signaling pathways guide the expression of 6TM-DOPr in these two species, and to model the physiology of human 6TM-DOPr in mice would present a challenge. This is supported by an earlier study demonstrating significant between-species differences in the expression and distribution of DOR-1 in the spinal cord and DRG in humans, rats, and mice using both in situ hybridization and radioligand binding [56]. To conclude, our results help expand the understanding of superficially explored and poorly understood aspects of the molecular biology of DOPrs and make the case for further studies to evaluate and harness the potential of DOPr isoforms as future drug targets.

Acknowledgements The authors would like to express their gratitude to Anna K. Naumova for her helpful comments and ideas. Cellecta Inc. is gratefully acknowledged for PCR on *OPRD1* transcripts in human tissues.

Funding Information This work was supported by The Canadian Institutes of Health Research (G237818/CERC09/CIHR to L.D.) and by the Intramural funds of the US Department of Health and Human Services to the National Library of Medicine (to S.A.S).

Compliance with Ethical Standards

Experimental procedures were approved by the Animal Care Committee at McGill University and conformed to the ethical guidelines of the Canadian Council of Animal Care and the guidelines of the Committee for Research and Ethical Issues of the International Association for the Study of Pain.

Conflict of Interest The authors declare that they have no conflict of interest.

References

1. Gendron L, Mittal N, Beaudry H, Walwyn W (2015) Recent advances on the delta opioid receptor: from trafficking to function. Br J Pharmacol 172:403–419. https://doi.org/10.1111/bph.12706
2. Pradhan AA, Smith ML, Zyuzin J, Charles A (2014) Delta-opioid receptor agonists inhibit migraine-related hyperalgesia, aversive state and cortical spreading depression in mice. Br J Pharmacol 171:2375–2384. https://doi.org/10.1111/bph.12591
3. Charles A, Pradhan AA (2016) Delta-opioid receptors as targets for migraine therapy. Curr Opin Neurol 29:314–319. https://doi.org/10.1097/WCO.0000000000000311
4. Vanderah TW (2010) Delta and kappa opioid receptors as suitable drug targets for pain. Clin J Pain 26(Suppl 10):S10–S15. https://doi.org/10.1097/AJP.0b013e3181c49e3a
5. Pradhan AA, Befort K, Nozaki C, Gaveriaux-Ruff C, Kieffer BL (2011) The delta opioid receptor: an evolving target for the treatment of brain disorders. Trends Pharmacol Sci 32:581–590. https://doi.org/10.1016/j.tips.2011.06.008
6. Gendron L, Cahill CM, von Zastrow M, Schiller PW, Pineyro G (2016) Molecular pharmacology of delta-opioid receptors. Pharmacol Rev 68:631–700. https://doi.org/10.1124/pr.114.008979
7. Petaja-Repo UE, Hogue M, Laperriere A, Walker P, Bouvier M (2000) Export from the endoplasmic reticulum represents the limiting step in the maturation and cell surface expression of the human delta opioid receptor. J Biol Chem 275:13727–13736. https://doi.org/10.1074/jbc.275.18.13727
8. Petaja-Repo UE, Hogue M, Leskela TT, Markkanen PM, Tuusa JT, Bouvier M (2006) Distinct subcellular localization for constitutive and agonist-modulated palmitoylation of the human delta opioid receptor. J Biol Chem 281:15780–15789. https://doi.org/10.1074/jbc.M602267200
9. Jiang Q, Takemori AE, Sultana M, Portoghese PS, Bowen WD, Mosberg HI, Porreca F (1991) Differential antagonism of opioid delta antinociception by [D-Ala2,Leu5,Cys6]enkephalin and naltrindole 5′-isothiocyanate: evidence for delta receptor subtypes. J Pharmacol Exp Ther 257:1069–1075
10. Dietis N, Rowbotham DJ, Lambert DG (2011) Opioid receptor subtypes: fact or artifact? Br J Anaesth 107:8–18. https://doi.org/10.1093/bja/aer115
11. Pasternak GW, Pan YX (2013) Mu opioids and their receptors: evolution of a concept. Pharmacol Rev 65:1257–1317. https://doi.org/10.1124/pr.112.007138
12. Convertino M, Samoshkin A, Gauthier J, Gold MS, Maixner W, Dokholyan NV, Diatchenko L (2015) Mu-opioid receptor 6-transmembrane isoform: a potential therapeutic target for new effective opioids. Prog Neuro-Psychopharmacol Biol Psychiatry 62:61–67. https://doi.org/10.1016/j.pnpbp.2014.11.009
13. Gaveriaux-Ruff C, Peluso J, Befort K, Simonin F, Zilliox C, Kieffer BL (1997) Detection of opioid receptor mRNA by RT-PCR reveals alternative splicing for the delta- and kappa-opioid receptors. Brain Res Mol Brain Res 48:298–304. https://doi.org/10.1016/S0169-328X(97)00109-5
14. Mayer P, Tischmeyer H, Jayasinghe M, Bonnekoh B, Gollnick H, Teschemacher H, Hollt V (2000) A delta opioid receptor lacking the third cytoplasmic loop is generated by atypical mRNA processing in human malignomas. FEBS Lett 480:156–160. https://doi.org/10.1016/S0304-3940(03)00382-3
15. Mayer P, Kroslak T, Tischmeyer H, Hollt V (2003) A truncated delta opioid receptor, spontaneously produced in human but not rat neuroblastoma cells, interferes with signaling of the full-length receptor. Neurosci Lett 344:62–64. https://doi.org/10.1016/S0014-5793(00)01929-3
16. Ogurtsov AY, Roytberg MA, Shabalina SA, Kondrashov AS (2002) OWEN: aligning long collinear regions of genomes. Bioinformatics 18:1703–1704
17. Edgar RC (2004) MUSCLE: multiple sequence alignment with high accuracy and high throughput. Nucleic Acids Res 32:1792–1797. https://doi.org/10.1093/nar/gkh340
18. Yang Z (2007) PAML 4: phylogenetic analysis by maximum likelihood. Mol Biol Evol 24:1586–1591. https://doi.org/10.1093/molbev/msm088
19. Michel AM, Fox G, Kiran A M, De Bo C, O'Connor PB, Heaphy SM, Mullan JP, Donohue CA et al (2014) GWIPS-viz: development of a ribo-seq genome browser. Nucleic Acids Res 42:D859–D864. https://doi.org/10.1093/nar/gkt1035
20. Maquat LE (2004) Nonsense-mediated mRNA decay: splicing, translation and mRNP dynamics. Nat Rev Mol Cell Biol 5:89–99. https://doi.org/10.1038/nrm1310
21. Choi HS, Kim CS, Hwang CK, Song KY, Wang W, Qiu Y, Law PY, Wei LN et al (2006) The opioid ligand binding of human mu-opioid receptor is modulated by novel splice variants of the receptor. Biochem Biophys Res Commun 343:1132–1140. https://doi.org/10.1016/j.bbrc.2006.03.084

22. Ingolia NT, Lareau LF, Weissman JS (2011) Ribosome profiling of mouse embryonic stem cells reveals the complexity and dynamics of mammalian proteomes. Cell 147:789–802. https://doi.org/10.1016/j.cell.2011.10.002
23. Dubot A, Godinot C, Dumur V, Sablonniere B, Stojkovic T, Cuisset JM, Vojtiskova A, Pecina P et al (2004) GUG is an efficient initiation codon to translate the human mitochondrial ATP6 gene. Biochem Biophys Res Commun 313:687–693. https://doi.org/10.1016/j.bbrc.2003.12.013
24. Sorek R (2007) The birth of new exons: mechanisms and evolutionary consequences. RNA 13:1603–1608. https://doi.org/10.1261/rna.682507
25. Hsu PY, Calviello L, Wu HL, Li FW, Rothfels CJ, Ohler U, Benfey PN (2016) Super-resolution ribosome profiling reveals unannotated translation events in Arabidopsis. Proc Natl Acad Sci U S A 113:E7126–E7135. https://doi.org/10.1073/pnas.1614788113
26. Werner A, Iwasaki S, McGourty CA, Medina-Ruiz S, Teerikorpi N, Fedrigo I, Ingolia NT, Rape M (2015) Cell-fate determination by ubiquitin-dependent regulation of translation. Nature 525:523–527. https://doi.org/10.1038/nature14978
27. Shabalina SA, Ogurtsov AY, Spiridonov NA, Koonin EV (2014) Evolution at protein ends: major contribution of alternative transcription initiation and termination to the transcriptome and proteome diversity in mammals. Nucleic Acids Res 42:7132–7144. https://doi.org/10.1093/nar/gku342
28. Shabalina SA, Spiridonov AN, Spiridonov NA, Koonin EV (2010) Connections between alternative transcription and alternative splicing in mammals. Genome Biol Evol 2:791–799. https://doi.org/10.1093/gbe/evq058
29. Yan Q, Weyn-Vanhentenryck SM, Wu J, Sloan SA, Zhang Y, Chen K, Wu JQ, Barres BA et al (2015) Systematic discovery of regulated and conserved alternative exons in the mammalian brain reveals NMD modulating chromatin regulators. Proc Natl Acad Sci U S A 112:3445–3450. https://doi.org/10.1073/pnas.1502849112
30. Shabalina SA, Zaykin DV, Gris P, Ogurtsov AY, Gauthier J, Shibata K, Tchivileva IE, Belfer I et al (2009) Expansion of the human mu-opioid receptor gene architecture: novel functional variants. Hum Mol Genet 18:1037–1051. https://doi.org/10.1093/hmg/ddn439
31. Ogurtsov AY, Marino-Ramirez L, Johnson GR, Landsman D, Shabalina SA, Spiridonov NA (2008) Expression patterns of protein kinases correlate with gene architecture and evolutionary rates. PLoS One 3:e3599. https://doi.org/10.1371/journal.pone.0003599
32. Shabalina SA, Ogurtsov AY, Spiridonov AN, Novichkov PS, Spiridonov NA, Koonin EV (2010) Distinct patterns of expression and evolution of intronless and intron-containing mammalian genes. Mol Biol Evol 27:1745–1749. https://doi.org/10.1093/molbev/msq086
33. Slavoff SA, Mitchell AJ, Schwaid AG, Cabili MN, Ma J, Levin JZ, Karger AD, Budnik BA et al (2013) Peptidomic discovery of short open reading frame-encoded peptides in human cells. Nat Chem Biol 9:59–64. https://doi.org/10.1038/nchembio.1120
34. D'Lima NG, Ma J, Winkler L, Chu Q, Loh KH, Corpuz EO, Budnik BA, Lykke-Andersen J et al (2017) A human microprotein that interacts with the mRNA decapping complex. Nat Chem Biol 13:174–180. https://doi.org/10.1038/nchembio.2249
35. Aebersold R, Agar JN, Amster IJ, Baker MS, Bertozzi CR, Boja ES, Costello CE, Cravatt BF et al (2018) How many human proteoforms are there? Nat Chem Biol 14:206–214. https://doi.org/10.1038/nchembio.2576
36. Starck SR, Ow Y, Jiang V, Tokuyama M, Rivera M, Qi X, Roberts RW, Shastri N (2008) A distinct translation initiation mechanism generates cryptic peptides for immune surveillance. PLoS One 3:e3460. https://doi.org/10.1371/journal.pone.0003460
37. Starck SR, Jiang V, Pavon-Eternod M, Prasad S, McCarthy B, Pan T, Shastri N (2012) Leucine-tRNA initiates at CUG start codons for protein synthesis and presentation by MHC class I. Science 336:1719–1723. https://doi.org/10.1126/science.1220270
38. Gerashchenko MV, Su D, Gladyshev VN (2010) CUG start codon generates thioredoxin/glutathione reductase isoforms in mouse testes. J Biol Chem 285:4595–4602. https://doi.org/10.1074/jbc.M109.070532
39. Studtmann K, Olschlager-Schutt J, Buck F, Richter D, Sala C, Bockmann J, Kindler S, Kreienkamp HJ (2014) A non-canonical initiation site is required for efficient translation of the dendritically localized Shank1 mRNA. PLoS One 9:e88518. https://doi.org/10.1371/journal.pone.0088518
40. Nilsen TW, Graveley BR (2010) Expansion of the eukaryotic proteome by alternative splicing. Nature 463:457–463. https://doi.org/10.1038/nature08909
41. Yeo G, Holste D, Kreiman G, Burge CB (2004) Variation in alternative splicing across human tissues. Genome Biol 5:R74. https://doi.org/10.1186/gb-2004-5-10-r74
42. Xu J, Xu M, Brown T, Rossi GC, Hurd YL, Inturrisi CE, Pasternak GW, Pan YX (2013) Stabilization of the mu-opioid receptor by truncated single transmembrane splice variants through a chaperone-like action. J Biol Chem 288:21211–21227. https://doi.org/10.1074/jbc.M113.458687
43. Samoshkin A, Convertino M, Viet CT, Wieskopf JS, Kambur O, Marcovitz J, Patel P, Stone LS et al (2015) Structural and functional interactions between six-transmembrane mu-opioid receptors and beta2-adrenoreceptors modulate opioid signaling. Sci Rep 5:18198. https://doi.org/10.1038/srep18198
44. Majumdar S, Grinnell S, Le Rouzic V, Burgman M, Polikar L, Ansonoff M, Pintar J, Pan YX et al (2011) Truncated G protein-coupled mu opioid receptor MOR-1 splice variants are targets for highly potent opioid analgesics lacking side effects. Proc Natl Acad Sci U S A 108:19778–19783. https://doi.org/10.1073/pnas.1115231108
45. Luco RF, Allo M, Schor IE, Kornblihtt AR, Misteli T (2011) Epigenetics in alternative pre-mRNA splicing. Cell 144:16–26. https://doi.org/10.1016/j.cell.2010.11.056
46. Zhou HL, Luo G, Wise JA, Lou H (2014) Regulation of alternative splicing by local histone modifications: potential roles for RNA-guided mechanisms. Nucleic Acids Res 42:701–713. https://doi.org/10.1093/nar/gkt875
47. Decosterd I, Woolf CJ (2000) Spared nerve injury: an animal model of persistent peripheral neuropathic pain. Pain 87:149–158. https://doi.org/10.1016/S0304-3959(00)00276-1
48. Massart R, Dymov S, Millecamps M, Suderman M, Gregoire S, Koenigs K, Alvarado S, Tajerian M et al (2016) Overlapping signatures of chronic pain in the DNA methylation landscape of prefrontal cortex and peripheral T cells. Sci Rep 6:19615. https://doi.org/10.1038/srep19615
49. Morinville A, Cahill CM, Esdaile MJ, Aibak H, Collier B, Kieffer BL, Beaudet A (2003) Regulation of delta-opioid receptor trafficking via mu-opioid receptor stimulation: evidence from mu-opioid receptor knock-out mice. J Neurosci 23:4888–4898. https://doi.org/10.1523/JNEUROSCI.23-12-04888.2003
50. Morinville A, Cahill CM, Aibak H, Rymar VV, Pradhan A, Hoffert C, Mennicken F, Stroh T et al (2004) Morphine-induced changes in delta opioid receptor trafficking are linked to somatosensory processing in the rat spinal cord. J Neurosci 24:5549–5559. https://doi.org/10.1523/JNEUROSCI.2719-03.2004
51. Pan YX, Xu J, Mahurter L, Bolan E, Xu M, Pasternak GW (2001) Generation of the mu opioid receptor (MOR-1) protein by three new splice variants of the Oprm gene. Proc Natl Acad Sci U S A 98:14084–14089. https://doi.org/10.1073/pnas.241296098
52. Gris P, Gauthier J, Cheng P, Gibson DG, Gris D, Laur O, Pierson J, Wentworth S et al (2010) A novel alternatively spliced isoform of the mu-opioid receptor: functional antagonism. Mol Pain 6:33. https://doi.org/10.1186/1744-8069-6-33

53. Convertino M, Samoshkin A, Viet CT, Gauthier J, Li Fraine SP, Sharif-Naeini R, Schmidt BL, Maixner W et al (2015) Differential regulation of 6- and 7-transmembrane helix variants of mu-opioid receptor in response to morphine stimulation. PLoS One 10: e0142826. https://doi.org/10.1371/journal.pone.0142826
54. Marrone GF, Le Rouzic V, Varadi A, Xu J, Rajadhyaksha AM, Majumdar S, Pan YX, Pasternak GW (2017) Genetic dissociation of morphine analgesia from hyperalgesia in mice. Psychopharmacology 234:1891–1900. https://doi.org/10.1007/s00213-017-4600-2
55. Oladosu FA, Conrad MS, O'Buckley SC, Rashid NU, Slade GD, Nackley AG (2015) Mu opioid splice variant MOR-1K contributes to the development of opioid-induced hyperalgesia. PLoS One 10: e0135711. https://doi.org/10.1371/journal.pone.0135711
56. Mennicken F, Zhang J, Hoffert C, Ahmad S, Beaudet A, O'Donnell D (2003) Phylogenetic changes in the expression of delta opioid receptors in spinal cord and dorsal root ganglia. J Comp Neurol 465:349–360. https://doi.org/10.1002/cne.10839